

Polynitrogen Chemistry. Synthesis, Characterization, and Crystal Structure of Surprisingly Stable Fluoroantimonate Salts of N_5^+

Ashwani Vij,[†] William W. Wilson,[†] Vandana Vij,[†] Fook S. Tham,[§] Jeffrey A. Sheehy,[†] and Karl O. Christe^{*,†,‡}

Contribution from the Propulsion Sciences and Advanced Concepts Division, Air Force Research Laboratory (AFRL/PR5), Edwards AFB, California 93524, Loker Hydrocarbon Research Institute and Department of Chemistry, University of Southern California, Los Angeles, California 90089, and Department of Chemistry, University of California, Riverside, California 92521

Received January 1, 2001. Revised Manuscript Received April 13, 2001

Abstract: The new N_5^+ salt, $N_5^+SbF_6^-$, was prepared from $N_2F^+SbF_6^-$ and HN_3 in anhydrous HF solution. The white solid is surprisingly stable, decomposing only at 70 °C, and is relatively insensitive to impact. Its vibrational spectrum exhibits all nine fundamentals with frequencies that are in excellent agreement with the theoretical calculations for a five-atomic V-shaped ion of C_{2v} symmetry. The $N_5^+Sb_2F_{11}^-$ salt was also prepared, and its crystal structure was determined. The geometry previously predicted for free gaseous N_5^+ from theoretical calculations was confirmed within experimental error. The $Sb_2F_{11}^-$ anions exhibit an unusual geometry with eclipsed SbF_4 groups due to interionic bridging with the N_5^+ cations. The N_5^+ cation is a powerful one-electron oxidizer. It readily oxidizes NO, NO_2 , and Br_2 but fails to oxidize Cl_2 , Xe, or O_2 .

Introduction

The recent discovery of $N_5^+AsF_6^-$ as a marginally stable compound that can be prepared on a macroscopic scale is quite remarkable.¹ The N_5^+ cation represented only the third readily accessible homonuclear polynitrogen species besides N_2 and N_3^- and as such has received much public acclaim.² Since N_5AsF_6 is only marginally stable and had given rise to some explosions,¹ it was of great interest to search for more stable N_5^+ salts in order to allow a more thorough characterization of this fascinating cation and to provide a suitable starting material for the pursuit of nitrogen allotropes. In this paper, the synthesis and characterization of surprisingly stable fluoroantimonate salts of N_5^+ and the crystal structure of $N_5^+Sb_2F_{11}^-$ are reported.

Experimental Section

Caution! HN_3 , azides, and polynitrogen compounds are highly endothermic and can decompose explosively. They should be handled only on a small scale with appropriate safety precautions (face shields, leather gloves, and protective clothing). Condensation of neat HN_3 at -196 °C into Teflon ampules containing oxidizers has repeatedly resulted in explosions upon condensation or melting of the HN_3 .

Materials and Apparatus. All reactions were carried out in 0.75-in.-o.d. Teflon-FEP or -PFA ampules that contained Teflon-coated magnetic stirring bars and were closed by stainless steel or Teflon valves. Volatile materials were handled on a stainless steel/Teflon-FEP vacuum line.³ Nonvolatile solids were handled in the dry nitrogen atmosphere of a glovebox. HN_3 was generated and handled on a Pyrex glass vacuum line equipped with grease-free Kontes glass/Teflon valves.

Infrared spectra were recorded on a Mattson Galaxy FT-IR spectrometer using dry powders pressed between AgCl windows in an Econo press (Barnes Engineering Co.). Raman spectra were recorded on a Bruker Equinox 55 FT-RA spectrometer using a Nd-YAG laser at 1064 nm and Pyrex melting point capillaries as sample containers. The thermal stabilities were determined using a DuPont model 910 DSC, crimp-sealed aluminum pans as sample containers, and heating rates of 3 °C/min. The data were recorded and analyzed with a DuPont model 2000 thermal analyst. Impact sensitivities were measured on an Olin Mathieson drop weight tester standardized with RDX (hexahydro-1,3,5-trinitro-1,3,5-triazine, 30 kg·cm, 50%).

The $N_2F^+SbF_6^-$ and $N_2F^+Sb_2F_{11}^-$ starting materials were prepared from *cis*- N_2F_2 and SbF_5 in anhydrous HF solution as previously described.^{4–7} The HF (Matheson Co.) was dried by storage over BiF_5 (Ozark Mahoning).⁸ The NO and NO_2 (Matheson Co) were purified by fractional condensation prior to their use. The O_2 and Xe (Matheson Co) were used as received. The preparation of HN_3 has previously been described.¹

Preparation of $N_5^+SbF_6^-$. A Teflon ampule, equipped with a stainless steel valve and containing a Teflon-coated magnetic stirring bar, was passivated with ClF_3 . It was attached to the metal vacuum line and treated several times with anhydrous HF until no color was observed upon freezing the HF at -196 °C. It was then loaded with $N_2F^+SbF_6^-$ (4.97 mmol) in the glovebox and attached to the metal vacuum line. The ampule was evacuated and cooled to -196 °C. Anhydrous HF (~2 mL) was then condensed into the ampule, and the contents were allowed to warm to ambient temperature with occasional stirring. After all the $N_2F^+SbF_6^-$ had dissolved, the ampule was recooled to -196 °C, and some additional neat HF was condensed onto the upper walls of the tube, where the HN_3 was going to be frozen out. The cold ampule was then connected to the glass line, and HN_3 (5.00 mmol)

[†] Air Force Research Laboratory.

[‡] University of Southern California.

[§] University of California, Riverside.

(1) Christe, K. O.; Wilson, W. W.; Sheehy, J. A.; Boatz, J. A. *Angew. Chem., Int. Ed.* **1999**, *38*, 2004.

(2) See, for example: *Chem. Eng. News* **1999**, *77*, Jan 25, 7; **1999**, *77*, Nov 29, 38; **2000**, *78*, Aug 14, 41.

(3) Christe, K. O.; Wilson, W. W.; Schack, C. J.; Wilson, R. D. *Inorg. Synth.* **1986**, *24*, 39.

(4) Ruff, J. K. *Inorg. Chem.* **1966**, *5*, 1971.

(5) Roesky, H. W.; Glemser, O.; Bormann, D. *Chem. Ber.* **1966**, *99*, 1589.

(6) Pankratov, V. A.; Savenkova, N. I. *Zh. Neorg. Khim.* **1968**, *13*, 2610.

(7) Christe, K. O.; Wilson, R. D.; Sawodny, W. *J. Mol. Struct.* **1971**, *8*, 245. Christe, K. O.; Wilson, R. D.; Wilson, W. W.; Bau, R.; Sukumar, S.; Dixon, D. A. *J. Am. Chem. Soc.* **1991**, *113*, 1991.

(8) Christe, K. O.; Wilson, W. W.; Schack, C. J. *J. Fluorine Chem.* **1978**, *11*, 71.

was added slowly at -196°C . The reaction mixture was allowed to warm slowly behind a safety shield to room temperature and kept at this temperature for about 45 min. The volatile materials were removed by pumping for several hours at 20°C , leaving behind a white powder (1.502 g, weight calculated for 4.97 mmol of $N_5SbF_6 = 1.520\text{ g}$) that was identified by its vibrational spectra as N_5SbF_6 .

This reaction was also carried out by first condensing HN_3 at -196°C into a passivated and preweighed Teflon ampule containing a known amount of HF. The resulting mixture was homogenized at ambient temperature. The ampule was taken into the glovebox, where a stoichiometric amount of $N_2F^+SbF_6^-$ was added at -196°C . The cold ampule was attached to the metal vacuum line and evacuated. Subsequent slow warming of the reaction mixture to room temperature for about 30 min, followed by removal of all volatile material, resulted in the isolation of $N_5^+SbF_6^-$ in $>99\%$ yield.

The safest method of generating HN_3 and reacting it with $N_2F^+SbF_6^-$ involved the use of two Teflon-FEP U-tubes that were interconnected through a porous Teflon filter (Pall Corp) and attached to the metal vacuum line. The first tube contained a weighed amount of NaN_3 and the second one a stoichiometric amount of $N_2F^+SbF_6^-$. Amounts of anhydrous HF, sufficient to dissolve both solids, were condensed at -196°C into both U-tubes, and the solids were dissolved in the HF at room temperature. The second U-tube, containing the $N_2F^+SbF_6^-$ solution, was cooled to -196°C , and the HN_3 , generated in the first U-tube, together with the excess of HF were co-condensed in a dynamic vacuum into the second U-tube. The resulting mixture was allowed to warm slowly to room temperature. Removal of the HF in a dynamic vacuum resulted in the isolation of very pure $N_5^+SbF_6^-$ in $>99\%$ yield. This procedure has been carried out repeatedly on a 5-g scale without incident.

Preparation of $N_5^+Sb_2F_{11}^-$. Freshly distilled SbF_5 (1.449 mmol) was added in the glovebox to a passivated Teflon-FEP ampule, and HF (1.9 mL liquid) was added on the metal vacuum line at -196°C . The mixture was homogenized at room temperature and taken back into the glovebox. The ampule was cooled inside the glovebox to -196°C and opened, and $N_5^+SbF_6^-$ (1.444 mmol) was added. The resulting mixture was allowed to warm to room temperature, and all volatile material was pumped off. The white solid residue (758 mg, weight calculated for 1.444 mmol of $N_5^+Sb_2F_{11}^- = 755\text{ mg}$) was shown by vibrational spectroscopy to consist of $N_5^+Sb_2F_{11}^-$.

Reactions of $N_5^+SbF_6^-$ with NO , NO_2 , O_2 , or Xe . In a typical experiment, a 0.5-in. Teflon-FEP ampule, that was closed by a Teflon valve, was loaded in the drybox with $N_5^+SbF_6^-$ (0.53 mmol). On the vacuum line, NO (4.2 mmol) was added at -196°C , and the contents of the ampule were allowed to warm slowly with intermittent cooling to room temperature. After the ampule was kept for 2 h at room temperature, it was cooled back to -196°C , and the volatile gas (1.34 mmol of N_2) was measured and pumped off. The unreacted NO was measured (3.6 mmol) and pumped off at room temperature, leaving behind 0.53 mmol of $NO^+SbF_6^-$ that was identified by vibrational spectroscopy.

In a similar manner, $N_5^+SbF_6^-$ was found to react quantitatively with NO_2 and Br_2 , but no reaction was observed with either Cl_2 , Xe , or O_2 .

Crystal Structure Determination of $N_5^+Sb_2F_{11}^-$. About 1 mL of anhydrous SO_2 was condensed onto 0.200 g of N_5SbF_6 at -196°C in a 0.5-in.-o.d. sapphire tube (Tyco Corp.) closed by a stainless steel valve. The contents of the tube were warmed to -78°C , causing all of the N_5SbF_6 to dissolve and form a pale yellowish solution. Anhydrous SO_2ClF ($\sim 1.5\text{ mL}$) was then slowly condensed onto this solution under vacuum. The solvents were then slowly removed under a static vacuum at -64°C over a period of $\sim 16\text{ h}$, leaving behind platelike colorless crystals. These crystals were extremely reactive to perfluoropolyether oil and showed an instantaneous evolution of nitrogen gas. The majority of the crystals were very soft and difficult to handle, but a few crystals appeared to exhibit a different habit and better mechanical strength. One of these crystals was immersed in halocarbon grease and mounted on the goniometer head using a precentered Nylon Cryoloop equipped with a magnetic base. The structure of the salt was determined using a Bruker diffractometer equipped with a CCD detector and a low-temperature, LT3, device. The three-circle platform with a fixed c -axis

Table 1. Crystal Data and Structure Refinement for $N_5^+Sb_2F_{11}^-$

| | |
|--------------------------------------|---|
| identification code | $N_5^+Sb_2F_{11}^-$ |
| empirical formula | $F_{11}N_5Sb_2$ |
| formula weight | 522.55 |
| temperature | 213(2) K |
| wavelength | 0.71073 Å |
| crystal system | monoclinic |
| space group | $C2/c$ |
| unit cell dimensions | $a = 10.913(8)\text{ Å}$, $\alpha = 90^\circ$ $b = 12.654(8)\text{ Å}$, $\beta = 104.715(18)^\circ$ $c = 16.675(11)\text{ Å}$, $\gamma = 90^\circ$ |
| volume | $2227(3)\text{ Å}^3$ |
| Z | 8 |
| density (calculated) | 3.117 Mg/m^3 |
| absorption coefficient | 4.995 mm^{-1} |
| $F(000)$ | 1888 |
| crystal size | $0.26 \times 0.10 \times 0.05\text{ mm}^3$ |
| θ range for data collection | $2.51\text{--}25.35^\circ$ |
| index ranges | $-12 \leq h \leq 13$ $-15 \leq k \leq 15$ $-20 \leq l \leq 17$ |
| reflections collected | 9125 |
| independent reflections | 2022 [$R(\text{int}) = 0.0629$] |
| absorption correction | SADABS |
| max. and min. transmission | 0.7883 and 0.3567 |
| refinement method | full-matrix least-squares on F^2 |
| data/restraints/parameters | 2022/0/164 |
| goodness-of-fit on F^2 | 1.122 |
| final R indices [$I > 2\sigma(I)$] | $R1 = 0.0678$, $wR2 = 0.1913$ |
| R indices (all data) | $R1 = 0.0785$, $wR2 = 0.2019$ |
| extinction coefficient | 0.00026(18) |
| largest diff. peak and hole | 4.329 and -2.102 e.Å^{-3} |

was controlled by the SMART⁹ software package. The unit cell parameters were determined at -60°C from three runs of data with 30 frames per run, using a scan speed of 30 s per frame. A complete hemisphere of data was collected, using 1271 frames at 30 s/frame, including 50 frames that were collected at the beginning and end of the data collection to monitor crystal decay. Data were integrated using the SAINT¹⁰ software package, and the raw data were corrected for absorption using the SADABS¹¹ program. The absence of $h + k = \text{odd}$ and $h0l$ reflections ($l = \text{odd}$) showed the presence of a C -centered lattice and a c -glide plane parallel and perpendicular to the b -axis, respectively, indicating Cc or $C2/c$ as the likely space groups. The intensity statistics, $E^2 - 1$ values, indicated a centrosymmetric space group, thereby excluding Cc as a possible space group. The space group was thus unambiguously assigned as $C2/c$. The structure was solved by the Patterson method using the SHELXS-97¹² program and refined by the least-squares method on F^2 using SHELXL-97.¹³ The initial Patterson map revealed the position of the two Sb atoms linked by a fluorine atom. The remaining atoms were located from subsequent difference electron density maps and finally refined anisotropically by the least-squares method on F^2 using the SHELXTL 5.1¹⁴ software for Windows NT. The crystal did not show any significant decomposition during the data collection. The experimental and refinement parameters are listed in Table 1.

Results and Discussion

Synthesis and Properties of $N_5^+SbF_6^-$. The synthesis of $N_5^+SbF_6^-$ was carried out in the same manner as previously reported¹ for $N_5^+AsF_6^-$ by reacting $N_2F^+SbF_6^-$ with HN_3 in

(9) SMART V 4.045, Software for the CCD Detector System, Bruker AXS, Madison, WI, 1999.

(10) SAINT V 4.035, Software for the CCD Detector System, Bruker AXS, Madison, WI, 1999.

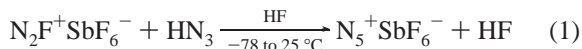
(11) SADABS, Program for absorption correction for area detectors, Version 2.01, Bruker AXS, Madison, WI, 2000.

(12) Sheldrick, G. M. SHELXS-97, Program for the Solution of Crystal Structure, University of Göttingen, Germany, 1997.

(13) Sheldrick, G. M. SHELXL-97, Program for the Refinement of Crystal Structure, University of Göttingen, Germany, 1997.

(14) SHELXTL 5.1 for Windows NT, Program library for Structure Solution and Molecular Graphics, Bruker AXS, Madison, WI, 1997.

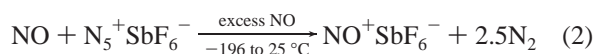
anhydrous HF solution at $-78\text{ }^{\circ}\text{C}$, followed by removal of the volatile products at room temperature. The yield of $\text{N}_5^+\text{SbF}_6^-$



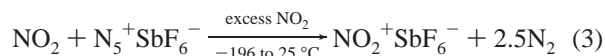
is essentially quantitative, and the product purity is high. It is essential that the reaction system is completely anhydrous, as water hydrolyzes the N_5^+ salt, generating free SbF_5 , which in combination with HF protonates HN_3 under formation of $\text{H}_2\text{N}_3^+\text{SbF}_6^-$.¹⁵

The $\text{N}_5^+\text{SbF}_6^-$ salt is a colorless hygroscopic solid that is stable at ambient temperature and, based on the DSC data, starts to decompose at $70\text{ }^{\circ}\text{C}$. It is surprisingly insensitive to impact. Even at the maximum setting of our apparatus ($200\text{ kg}\cdot\text{cm}$), only partial thermal decomposition due to adiabatic heating of the sample was observed, but no explosions. The salt is soluble in and compatible with HF, SO_2 , and CHF_3 .

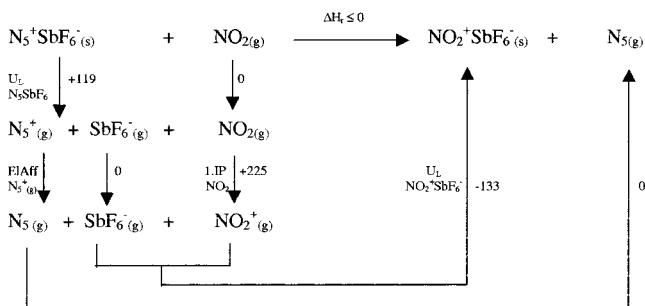
The oxidizing properties of $\text{N}_5^+\text{SbF}_6^-$ were examined in the solid state and in HF solution by treating it with 2 atm of either oxygen or xenon gas between $-78\text{ }^{\circ}\text{C}$ and ambient temperature. No oxidations to O_2^+ and Xe_2^+ , respectively, were observed under these conditions. Furthermore, solid $\text{N}_5^+\text{SbF}_6^-$ did not oxidize liquid or gaseous chlorine, but is capable of oxidizing NO (2), NO_2 (3), and Br_2 .



and



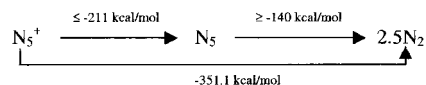
Since NO, NO_2 , Br_2 , Cl_2 , O_2 , and Xe have first ionization potentials of 9.26, 9.75, 10.52, 11.48, 12.07, and 12.13 eV, respectively, these experiments indicate that the N_5^+ cation can oxidize substrates having a first ionization potential of 10.52 eV or less, but cannot oxidize substrates with a first ionization potential of 11.48 eV or more. When solid starting materials or reaction products are involved in these redox reactions, the first ionization potential of the substrate does not equal the electron affinity of the oxidizing agent, as any lattice energy changes must also be taken into account. For the calculation of the electron affinity, the appropriate Born–Haber cycle must be used, as shown in kilocalories per mole for reaction (3).



For the redox reaction to proceed, the enthalpy change, or more precisely the free energy change if entropy changes are included, of the reaction must be negative. Assuming ΔH_r to be zero, the electron affinity of $\text{N}_5^+(g)$ is calculated to have a minimum value of 211 kcal/mol or 9.16 eV, a value significantly lower than the first ionization potential of NO_2 (9.75 eV). The required

(15) Christe, K. O.; Wilson, W. W.; Dixon, D. A.; Khan, S. I.; Bau, R.; Metzenthin, T.; Lu, R. *J. Am. Chem. Soc.* **1993**, *115*, 1836.

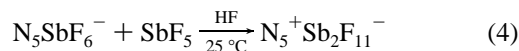
and experimentally unknown lattice energy values for N_5SbF_6 and NO_2SbF_6 were estimated using the method¹⁶ of Jenkins and Passmore based on Bartlett's volume-based relationship.¹⁷ It should be kept in mind, however, that the structure of $\text{N}_{5(g)}$ is unknown and that the final reaction product is 2.5 mol of N_2 . The conversion of N_5 to N_2 is also strongly exothermic, as is apparent from the calculated¹ heat of formation of gaseous N_5^+ (351.1 kcal/mol) and the above-derived minimum electron affinity value of N_5^+ (211 kcal/mol).



The above results show that N_5^+ is a weaker oxidizer than either PtF_6 that can oxidize O_2 to O_2^+ ¹⁸ or O_2^+ that can oxidize Xe to Xe_2^+ under similar conditions.^{19,20} Despite the first ionization potential (IP) of N_2 (15.51 eV) being 3.44 eV higher than that of O_2 (12.07 eV), the electron affinity of N_5^+ is substantially lower than that of O_2^+ because in N_5^+ the positive charge is spread over a larger number of atoms, thereby decreasing its oxidizing power. Nevertheless, the fact that N_5^+ can quantitatively oxidize either NO, NO_2 , or Br_2 renders it a very strong one-electron oxidizer. Although it is not quite as powerful as PtF_6 or O_2^+ salts, it offers the great advantage of not acting as a fluorinating or oxygenating agent, which can be a very important consideration when dealing with substrates that are easily fluorinated or oxygenated.

Ongoing studies in our laboratory show that the potential hazards of handling neat HN_3 in the synthesis of N_5^+ can be avoided by either replacing HN_3 with the insensitive $(\text{CH}_3)_3\text{SiN}_3$ or generating the desired HN_3 from a weighed amount of NaN_3 and excess HF in a separate ampule and transferring all volatiles into the reaction vessel containing an HF solution of $\text{N}_2\text{F}^+\text{SbF}_6^-$. The reactions with $(\text{CH}_3)_3\text{SiN}_3$ are carried out in either HF or SO_2 solution and produce N_5^+ in high yield. When HF is used as the solvent, the first reaction step most certainly involves the formation of $(\text{CH}_3)_3\text{SiF}$ and HN_3 ; i.e., HN_3 is generated in situ in the reactor.

Synthesis and Properties of $\text{N}_5^+\text{Sb}_2\text{F}_{11}^-$. To preclude a potential side reaction of $\text{Sb}_2\text{F}_{11}^-$ with HF and HN_3 to give SbF_6^- and $\text{H}_2\text{N}_3^+\text{SbF}_6^-$, a sample of $\text{N}_5^+\text{SbF}_6^-$ was reacted with an equimolar amount of SbF_5 in HF solution at room temperature. The resulting $\text{N}_5^+\text{Sb}_2\text{F}_{11}^-$ salt is a colorless solid



that is stable at room temperature and undergoes, according to its DSC data, thermal decomposition at $70\text{ }^{\circ}\text{C}$; i.e., its thermal stability is comparable to that of $\text{N}_5^+\text{SbF}_6^-$, but, in contrast to $\text{N}_5^+\text{SbF}_6^-$, it undergoes a reversible endotherm (melting) at about $30\text{ }^{\circ}\text{C}$. Consequently, the replacement of SbF_6^- by $\text{Sb}_2\text{F}_{11}^-$ did not result in increased thermal stability and does not appear to offer any significant advantages for studying the reaction chemistry of N_5^+ salts.

Crystal Structure of $\text{N}_5^+\text{Sb}_2\text{F}_{11}^-$. The structure of $\text{N}_5^+\text{Sb}_2\text{F}_{11}^-$ is shown in Figures 1 and 2, and the important bond lengths

(16) Jenkins, H. D. B.; Roobottom, H. K.; Passmore, J.; Glasser, L. *Inorg. Chem.* **1999**, *38*, 3609.

(17) Mallouk, T. E.; Rosenthal, G. L.; Muller, G.; Busasco, R.; Bartlett, N. *Inorg. Chem.* **1984**, *23*, 3167.

(18) Bartlett, N.; Lohmann, D. H. *Proc. R. Chem. Soc. (London)* **1962**, *277*; *J. Chem. Soc.* **1962**, 5253.

(19) Stein, L.; Norris, J. R.; Downs, A. J.; Minihan, A. R. *J. Chem. Soc., Chem. Commun.* **1978**, 502.

(20) Stein, L.; Henderson, W. W. *J. Am. Chem. Soc.* **1980**, *102*, 2856.

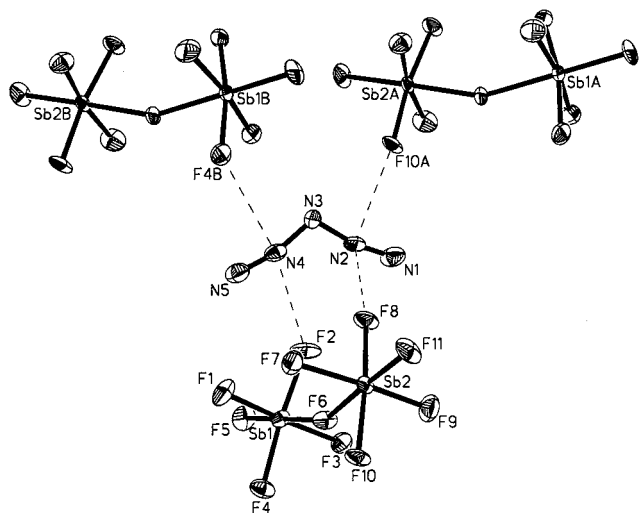


Figure 1. ORTEP diagram of $N_5^+Sb_2F_{11}^-$, showing the thermal ellipsoids at the 30% probability level and the close-range $N \cdots F$ contacts within the crystal lattice.

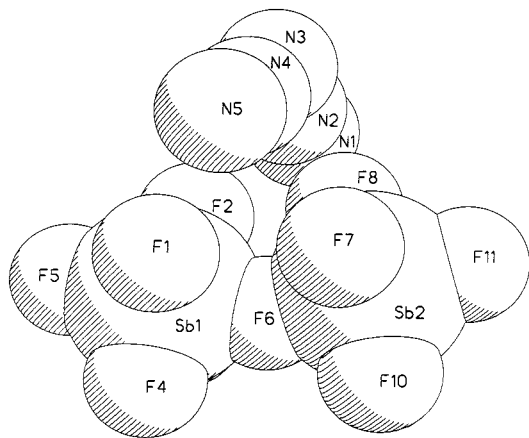


Figure 2. Space-filling representation of $N_5^+Sb_2F_{11}^-$, showing the close packing of the N_5^+ cation within the $Sb_2F_{11}^-$ cavity.

and angles are summarized in Table 2. The observed V-shaped geometry of the N_5^+ cation is in excellent agreement with the theoretical predictions¹ for the free gaseous N_5^+ cation at the B3LYP level of theory, with the calculated terminal and central N–N bond distances of 1.11 and 1.30 Å being close to the observed values of 1.105(19) and 1.299(19) Å, respectively. Furthermore, the terminal N–N distance of 1.105(19) Å in N_5^+ is only slightly longer than that of 1.089(9) Å found for N_2F^+ in $N_2F^+Sb_2F_{11}^-$ ²¹ and compares well with the N–N bond distances of 1.0976(2) Å in N_2 ²² and 1.0927 Å found in HN_2^+ ,^{23,24} indicating that the terminal bonds approximate triple bonds. The central N–N bond length of 1.299(19) Å in N_5^+ is somewhat longer than typical N–N double bonds (1.17–1.25 Å) but is significantly shorter than typical N–N single bonds (1.43–1.75 Å).²⁵ Additionally, the agreement between calculated [112.3 and 166.7°] and observed [111.2(11) and 167.2(15)°, respectively] bond angles is very good.

(21) Vij, A.; Vij, V.; Tham, F.; Christe, K. O. Unpublished results.

(22) Huber, K. P.; Herzberg, G. *Constants of Diatomic Molecules*; Van Nostrand Reinhold: New York, 1979.

(23) Owrutsky, J. C.; Gudeman, C. S.; Martner, C. C.; Tack, L. M.; Rosenbaum, N. H.; Saykally, R. J. *J. Phys. Chem.* **1986**, *84*, 605.

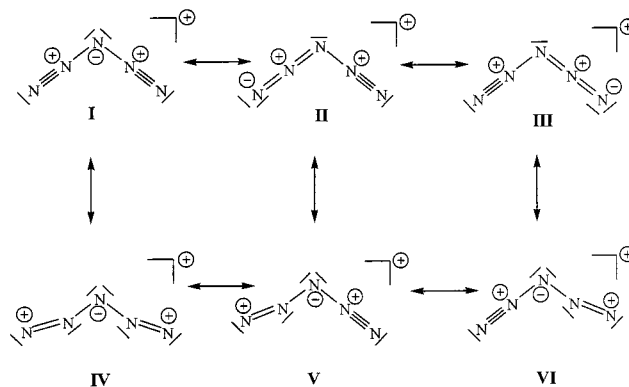
(24) Botschwina, P. *Chem. Phys. Lett.* **1984**, *107*, 535.

(25) Greenwood, N. N.; Earnshaw, A. *Chemistry of the Elements*, 2nd ed.; Butterworth, Heinemann: Oxford, 1998.

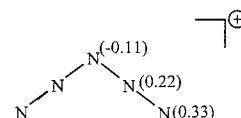
Table 2. Bond Lengths and Angles for $N_5^+Sb_2F_{11}^-$

| Bond Lengths (Å) | | | |
|-------------------|-----------|-------------------|-----------|
| Sb(1)–F(5) | 1.839(8) | Sb(2)–F(9) | 1.849(10) |
| Sb(1)–F(4) | 1.845(8) | Sb(2)–F(8) | 1.866(8) |
| Sb(1)–F(2) | 1.851(9) | Sb(2)–F(11) | 1.866(8) |
| Sb(1)–F(3) | 1.854(9) | Sb(2)–F(6) | 2.007(7) |
| Sb(1)–F(1) | 1.856(10) | N(1)–N(2) | 1.102(19) |
| Sb(1)–F(6) | 2.031(7) | N(2)–N(3) | 1.303(19) |
| Sb(2)–F(10) | 1.844(7) | N(3)–N(4) | 1.295(19) |
| Sb(2)–F(7) | 1.849(9) | N(4)–N(5) | 1.107(19) |
| Bond Angles (deg) | | | |
| F(5)–Sb(1)–F(2) | 94.8(4) | F(7)–Sb(2)–F(9) | 170.7(5) |
| F(4)–Sb(1)–F(2) | 169.9(4) | F(10)–Sb(2)–F(8) | 171.3(4) |
| F(5)–Sb(1)–F(3) | 95.4(5) | F(7)–Sb(2)–F(8) | 87.9(4) |
| F(4)–Sb(1)–F(3) | 89.7(4) | F(9)–Sb(2)–F(8) | 88.8(5) |
| F(2)–Sb(1)–F(3) | 89.3(5) | F(10)–Sb(2)–F(11) | 94.8(4) |
| F(5)–Sb(1)–F(1) | 93.6(5) | F(7)–Sb(2)–F(11) | 96.7(5) |
| F(4)–Sb(1)–F(1) | 91.0(5) | F(9)–Sb(2)–F(11) | 92.2(5) |
| F(2)–Sb(1)–F(1) | 88.4(5) | F(8)–Sb(2)–F(11) | 93.9(4) |
| F(3)–Sb(1)–F(1) | 170.8(4) | F(10)–Sb(2)–F(6) | 85.0(3) |
| F(5)–Sb(1)–F(6) | 179.9(5) | F(7)–Sb(2)–F(6) | 85.9(4) |
| F(4)–Sb(1)–F(6) | 84.7(4) | F(9)–Sb(2)–F(6) | 85.3(5) |
| F(2)–Sb(1)–F(6) | 85.1(4) | F(8)–Sb(2)–F(6) | 86.3(4) |
| F(3)–Sb(1)–F(6) | 84.5(4) | F(11)–Sb(2)–F(6) | 177.5(4) |
| F(1)–Sb(1)–F(6) | 86.4(4) | Sb(2)–F(6)–Sb(1) | 155.0(4) |
| F(10)–Sb(2)–F(7) | 91.2(5) | N(1)–N(2)–N(3) | 168.1(15) |
| F(10)–Sb(2)–F(9) | 90.8(5) | N(4)–N(3)–N(2) | 111.2(11) |

The observed geometry supports the previously given rationale¹ that the exceptional stability of N_5^+ is largely due to resonance stabilization, resulting in relatively high bond orders for all the bonds. The bonding in N_5^+ can be described by the following six resonance structures:



Although structures **IV–VI** possess one or two terminal nitrogen atoms with only six valence electrons, it must be kept in mind that conventional Lewis structures are oversimplifications and often do not adequately describe the actual bonding. Inclusion of structures **IV–VI** is required to account for the charge distributions calculated at the NBO(B3LYP/aug-cc-pVDZ) level,²⁶



as well as the relative shielding of the N NMR signals (the shielding increases from the terminal nitrogen to the β -nitrogen to the central nitrogen)¹ and the terminal N–N–N bond angles of about 167°.

A least-squares plane analysis for N_5^+ shows that the cation is essentially planar. The N2 atom exhibits a maximum deviation of 0.11 Å from the average mean plane that shows a root-mean-

(26) Fau, S.; Bartlett, R. J. *J. Phys. Chem. A* **2001**, *105*, 4096.

Table 3. Observed Infrared and Raman Spectra of $N_5^+SbF_6^-$, $N_5^+Sb_2F_{11}^-$ and $N_5^+AsF_6^-$ and Their Assignments

| observed frequency (cm^{-1}) and relative intensity | | | | | | assignments (point group) | | |
|---|------------|-----------------------|--|----------------|---------------|---------------------------------------|---------------------|----------------|
| $N_5^+SbF_6^-$ | | $N_5^+Sb_2F_{11}^-$ | | $N_5^+AsF_6^-$ | | N_5^+ (C_{2v}) | SbF_6^- (O_h) | $Sb_2F_{11}^-$ |
| IR | Raman | IR | Raman | IR | Raman | | | |
| 3357 vw | | | | | | $(\nu_1 + \nu_3 + \nu_9)(B_2) = 3358$ | | |
| 3334 vw | | | | | | $(\nu_1 + \nu_8)(B_2) = 3323$ | | |
| 3079 w | | 3069 w | | | | $(\nu_2 + \nu_7)(B_2) = 3077$ | | |
| 2681 vw | | 2671 vw | | | | $(\nu_1 + \nu_9)(B_2) = 2682$ | | |
| 2270 m | 2268 (9.4) | 2260 m | 2261 (9.0) | 2270 m | 2271 (4.4) | $(\nu_1)(A_1)$ | | |
| 2205 s | 2205 (2.0) | 2203 s | 2202 (1.9) | 2210 s | 2211 (0.8) | $(\nu_7)(B_2)$ | | |
| 1921 vw | | 1919 vw | | | | $(\nu_3 + 3\nu_9)(B_2) = 1914$ | | |
| 1891 vw | | 1883 vw | | | | $(\nu_8 + 2\nu_9)(B_2) = 1883$ | | |
| 1240 vw | | 1366 w } 1288 vw } | | | | | comb. bands | comb. bands |
| 1092 ms | | 1089 s | | 1088 s | | $(\nu_3 + \nu_9)(B_2) = 1086^a$ | | |
| 1064 s | | 1064 s | | | | $\nu_8(B_2)$ | | |
| 902 vvw | | 892 vvw | | | | $(\nu_5 + \nu_6)(B_2) = 903$ | | |
| 871 w | 872 (0.6) | 867 w | 866 (0.6) | 872 w | 871 (0.7) | $\nu_2(A_1)$ | | |
| 835 vw | 837 (0+) | 824 vw | 824 (0+) | | | $(2\nu_9)(A_1) = 828^b$ | | |
| | | 725–650 vs,br | 692 (5.5) } 654 (10) } 598 (1.4) } | | | | | νSbF |
| 655 vs | 672 (1) | | 664 (~1) | 680 sh | 669/672 (1.8) | $\nu_3(A_1)$ | | |
| | 652 (10) | | | 704 vs | | | $\nu_3(F_{1u})$ | |
| | | 596 mw } 537 mw } | | | | | $\nu_1(A_{1g})$ | νSbF |
| 582 w | 571 (0.8) | | | 575 w | 579 (1.6) | | $\nu_2(E_g)$ | $\nu Sb-F-Sb$ |
| | 478 (0+) | 497 s | 470 (0+) | | | | | |
| 447 w | | 449 w | | | | $\nu_5(A_2)$ | | |
| 425 ms | | 417 ms | | 420 sh | | ? | | |
| 412 mw | 416 (0+) | 409 sh | 417 (0+) | | | $\nu_6(B_1)$ | | |
| | | | 295 (2.1) } 283 sh } 272 sh } 231 (2.0) } | | | $\nu_9(B_2)$ | | $\delta Sb-F$ |
| 284 vs | | | | 394 vs | | | $\nu_4(F_{1u})$ | |
| | 282 (2.8) | | | | | | $\nu_5(F_{2g})$ | |
| | 204 (5.0) | | 200 (3.6) | | 372 (3.4) | | | |
| | 107 (5) | | 135 sh } 97 (5.0) } | | 209 (4.4) | $\nu_4(A_1)$ | | |
| | | | | | 125 (5.5) | lattice vibrations | | |

^a In Fermi resonance with $\nu_8(B_2)$. ^b In Fermi resonance with $\nu_2(A_1)$.

square deviation of 0.0058 Å. The N_5^+ mean plane is almost perpendicular (78.1°) to the plane containing the F5–Sb1–F6–Sb2–F11 atoms. The latter is also almost perfectly planar and shows a root-mean-square deviation of 0.014 Å.

The geometry of the $Sb_2F_{11}^-$ anion also deserves special comment. This anion is known to possess little rigidity and can exist in either an eclipsed or a staggered conformation and exhibit a wide range of Sb–F–Sb bridge angles, depending upon the counterion present in the crystal lattice.²⁷ The eclipsed conformation is rare but has previously also been observed for $BrF_4^+Sb_2F_{11}^-$.²¹ In the latter compound, the eclipsed structure results from a packing effect in which one equatorial fluorine ligand of each antimony atom of $Sb_2F_{11}^-$ bridges to a different BrF_4^+ cation. Since the two BrF_4^+ cations and the $Sb_2F_{11}^-$ anion are coplanar, the bridging equatorial fluorine ligands around the antimonies become also coplanar, resulting in the eclipsed configuration. The eclipsed conformation of the $Sb_2F_{11}^-$ anion found for $N_5^+Sb_2F_{11}^-$ is also due to fluorine bridging²⁸ but

(27) Willner, H.; Bodenbinder, M.; Broechler, R.; Hwang, G.; Rettig, S. J.; Trotter, J.; von Ahsen, B.; Westphal, U.; Jonas, V.; Thiel, W.; Aubke, F. *J. Am. Chem. Soc.* **2001**, *123*, 588.

(28) $N_5^+Sb_2F_{11}^-$ shows numerous $N\cdots F$ contacts shorter than the sum of the van der Waals radii of 3.0 Å. The shortest contacts, 2.723(15) and 2.768(14) Å, arise from $N2\cdots F8$ and $N2\cdots F10^a$ ($a = 1/2 + x, 1/2 - y, 1/2 + z$), while the $N4\cdots F2$ and $N4\cdots F4^b$ ($b = x, 1 - y, 3/2 - z$) distances, 2.887(15) and 2.813 Å, respectively, are slightly longer.

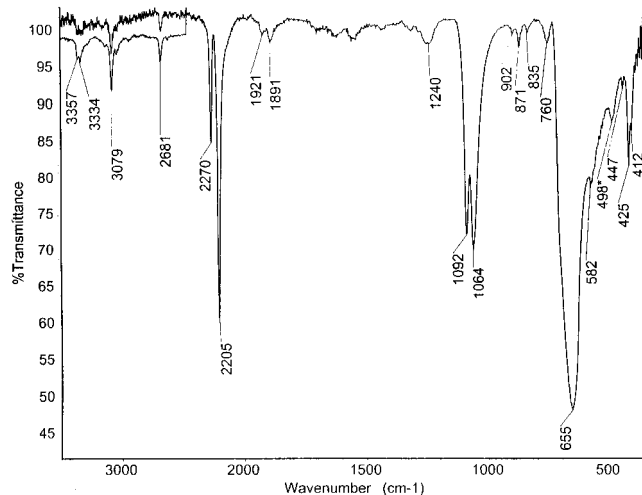


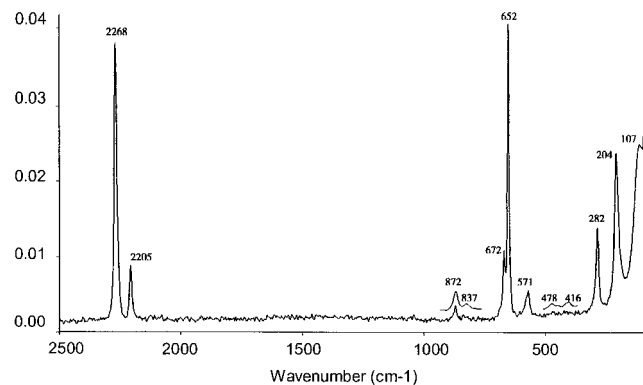
Figure 3. Infrared spectrum of solid $N_5^+SbF_6^-$, recorded as an AgBr pellet at room temperature. The band at 493 cm^{-1} , marked by an asterisk, is due to a small amount of $Sb_2F_{11}^-$.

results from N_5^+ acting as a spacer between the two equatorial SbF_4 units of $Sb_2F_{11}^-$ (Figure 2). In accord with the resonance structures and the calculated charge distributions of N_5^+ (see above), the positively charged nitrogen atoms interact with the

Table 4. Comparison of Observed and Unscaled Calculated CCSD(T)/6-311+G(2d) Vibrational Frequencies (cm^{-1}) and Intensities (km mol^{-1} and $\text{\AA}^4 \text{amu}^{-1}$) for N_5^+

| | approx mode description in point group C_{2v} | calcd freq | abs int | | obsd freq | rel int | |
|----------------|---|------------|---------|-------|-----------|----------------|----------------|
| | | | IR | Raman | | IR | Raman |
| A ₁ | ν_1 in-phase terminal stretches | 2229 | 13 | 215 | 2260–2271 | m | 10.0 |
| | ν_2 sym central stretch | 818 | 0.5 | 5 | 866–872 | w | 0.6 |
| | ν_3 central bending | 644 | 2 | 1 | 664–672 | obscd | 1 ^a |
| | ν_4 in-phase terminal bends | 181 | 0.3 | 6 | 200–209 | — ^b | 4 |
| A ₂ | ν_5 out-of-phase, out-of-plane bend | 475 | 0 | 1 | 470–478 | — | 0+ |
| B ₁ | ν_6 in-phase, out-of-plane bend | 405 | 6 | 0 | 417–425 | ms | 0 |
| B ₂ | ν_7 out-of-phase term stretches | 2175 | 105 | 42 | 2203–2211 | s | 1.9 |
| | ν_8 asym central stretch | 1032 | 138 | 2 | 1055–1064 | s | not obsd |
| | ν_9 out-of-phase term bends | 399 | 1 | 0.5 | 412–417 | mw | 0+ |

^a Obscured in infrared and interference in Raman by anion bands. ^b Outside of the frequency range of our spectrometer.

**Figure 4.** Raman spectrum of solid $N_5^+SbF_6^-$ recorded at room temperature.

negatively charged fluorine ligands (Figure 1). Thus, the β -nitrogens, N2 and N4, bridge to the two eclipsed fluorine atoms, F2 and F8, but since the N_5^+ plane is not perfectly perpendicular to the $F_{ax}-Sb-F-Sb-F_{ax}$ plane, the N2–F8 and N4–F2 distances are somewhat shorter than the N2–F2 and N4–F8 distances.²⁸ In contrast to $BrF_4^+Sb_2F_{11}^-$, which has an almost linear Sb–F–Sb bridge angle of 175° ,²¹ that of $155.0(4)^\circ$ in $N_5^+Sb_2F_{11}^-$ is much closer to those usually found for $Sb_2F_{11}^-$.²⁷

Vibrational Spectra of N_5^+ . The infrared and Raman spectra of solid $N_5^+SbF_6^-$ are shown in Figures 3 and 4, respectively. The experimentally observed frequencies of $N_5^+SbF_6^-$, $N_5^+Sb_2F_{11}^-$, and $N_5^+AsF_6^-$, together with their assignments, are listed in Table 3. A comparison of the observed and calculated frequencies and intensities of N_5^+ is given in Table 4. As can be seen, the previously missing¹ remaining four fundamental vibrations and numerous combination bands of N_5^+ have been observed and are in excellent agreement with the theoretical

predictions for point group C_{2v} . The splittings observed for ν_8 –(B₂) and ν_2 (A₁) can be attributed to Fermi resonance. The presence of $Sb_2F_{11}^-$ impurities in the SbF_6^- salt can be readily detected by Raman bands at 692, 598, and 231 cm^{-1} and infrared bands at 708 and 497 cm^{-1} that are characteristic for $Sb_2F_{11}^-$ and do not overlap with the SbF_6^- bands.

Conclusion

The synthesis and thorough characterization of $N_5^+SbF_6^-$ and $N_5^+Sb_2F_{11}^-$ demonstrate that the N_5^+ cation can form exceptionally stable salts with fluoroantimonate anions and that these salts are surprisingly insensitive to impact. The N_5^+ cation is a powerful one-electron oxidizer that can oxidize NO, NO₂, and Br₂ and does not give rise to undesirable fluorination or oxygenation side reactions. The ready availability of a stable polynitrogen cation in addition to the long-known azide anion opens a venue to neutral polynitrogen compounds and may provide the basis for the first synthesis of stable nitrogen allotropes.

Acknowledgment. The authors thank the Defense Advanced Research Project Agency, the U.S. Air Force Office of Scientific Research, and the National Science Foundation for financial support and Drs. T. Schroer, S. Schneider, and M. Gerken from the University of Southern California for experimental support and stimulating discussions.

Supporting Information Available: Tables of structure determination summary, atomic coordinates, bond lengths and angles, and anisotropic displacement parameters of $N_5Sb_2F_{11}$ (PDF). This material is available free of charge via the internet at <http://pubs.acs.org>.

JA010141G